

Angle resolved photoelectron spectroscopy of two-color XUV–NIR ionization with polarization control

This content has been downloaded from IOPscience. Please scroll down to see the full text.

2016 J. Phys. B: At. Mol. Opt. Phys. 49 165003

(<http://iopscience.iop.org/0953-4075/49/16/165003>)

View [the table of contents for this issue](#), or go to the [journal homepage](#) for more

Download details:

IP Address: 134.76.223.157

This content was downloaded on 26/09/2016 at 14:31

Please note that [terms and conditions apply](#).

You may also be interested in:

[Interference in the angular distribution of photoelectrons in superimposed XUV and optical laser fields](#)

S Dusterer, L Rading, P Johnsson et al.

[Atomic photoionization in combined intense XUV free-electron and infrared laser fields](#)

P Radcliffe, M Arbeiter, W B Li et al.

[Two-colour experiments in the gas phase](#)

M Meyer, J T Costello, S Dusterer et al.

[Femtosecond x-ray pulse length characterization at the Linac Coherent Light Source free-electron laser](#)

S Dusterer, P Radcliffe, C Bostedt et al.

[Dichroism in the above-threshold two-colour photoionization of singly charged neon](#)

V Richardson, W B Li, T J Kelly et al.

[Circular dichroism in XUV + IR multiphoton ionization of atoms](#)

A K Kazansky, A V Bozhevolnov, I P Sazhina et al.

Angle resolved photoelectron spectroscopy of two-color XUV–NIR ionization with polarization control

S Düsterer¹, G Hartmann¹, F Babies², A Beckmann², G Brenner¹, J Buck², J Costello³, L Dammann¹, A De Fanis², P Geßler², L Glaser¹, M Ilchen^{2,4}, P Johnsson⁵, A K Kazansky^{6,7,8}, T J Kelly³, T Mazza², M Meyer², V L Nosik^{9,10}, I P Sazhina¹¹, F Scholz¹, J Seltmann¹, H Sotoudi², J Viefhaus¹ and N M Kabachnik^{2,11}

¹Deutsches Elektronen-Synchrotron (DESY), Notkestrasse 85, D-22603 Hamburg, Germany

²European XFEL GmbH, Holzkoppel 4, 22869 Schenefeld, Germany

³National Center for Plasma Science and Technology and School of Physical Sciences, Dublin City University, Dublin, Ireland

⁴PULSE at Stanford, 2575 Sand Hill Road, Menlo Park, CA 94025, USA

⁵Lund University, PO Box 118, SE-221 00 Lund, Sweden

⁶Departamento de Física de Materiales, University of the Basque Country UPV/EHU, E-20018 San Sebastian/Donostia, Spain

⁷Donostia International Physics Center (DIPC), E-20018 San Sebastian/Donostia, Basque Country, Spain

⁸IKERBASQUE, Basque Foundation for Science, E-48011 Bilbao, Spain

⁹National Research Centre 'Kurchatov Institute', Moscow, Russia

¹⁰National Research Nuclear University 'Moscow Engineering Physical Institute', Moscow, Russia

¹¹Skobeltsyn Institute of Nuclear Physics, Lomonosov Moscow State University, Moscow 119991, Russia

E-mail: stefan.duesterer@desy.de

Received 22 March 2016, revised 20 June 2016

Accepted for publication 23 June 2016

Published 4 August 2016



CrossMark

Abstract

Electron emission caused by extreme ultraviolet (XUV) radiation in the presence of a strong near infrared (NIR) field leads to multiphoton interactions that depend on several parameters. Here, a comprehensive study of the influence of the angle between the polarization directions of the NIR and XUV fields on the two-color angle-resolved photoelectron spectra of He and Ne is presented. The resulting photoelectron angular distribution strongly depends on the orientation of the NIR polarization plane with respect to that of the XUV field. The prevailing influence of the intense NIR field over the angular emission characteristics for He(1s) and Ne(2p) ionization lines is shown. The underlying processes are modeled in the frame of the strong field approximation (SFA) which shows very consistent agreement with the experiment reaffirming the power of the SFA for multicolor-multiphoton ionization in this regime.

Keywords: photoionization, two-color multiphoton interaction, photoelectron angular distribution

(Some figures may appear in colour only in the online journal)

1. Introduction

Free-electron lasers (FELs) working in the extreme ultraviolet (XUV) and x-ray region deliver unrivaled intense pulses of fs-duration [1–4]. They allow for investigations of basic

 Original content from this work may be used under the terms of the [Creative Commons Attribution 3.0 licence](https://creativecommons.org/licenses/by/3.0/). Any further distribution of this work must maintain attribution to the author(s) and the title of the work, journal citation and DOI.

light–matter interaction at high photon intensity such as multiphoton ionization of atoms and molecules. Especially at high photon energy, both inner shell and valence electrons can be ionized which yields deep insight into fundamental physical properties and processes [5–7]. The combination of femtosecond XUV pulses with optical or near infrared (NIR) laser pulses of similar duration enables, not only dynamical studies, but also investigations of simultaneous two-color interactions with such small quantum systems. XUV–NIR multiphoton absorption in atoms has progressively yielded new insights in this complex topic (see overview [8] and references therein). Ionization by the XUV pulse creates electrons with typically a few tens of eV kinetic energy and a narrow kinetic energy distribution. The additional absorption or emission of NIR photons leads to a modulation of the photoelectron spectrum resulting in additional lines spaced by the photon energy of the optical or NIR photon (typically a few eV) [9]. These additional lines are called ‘sidebands’. The monochromaticity of the FELs makes it possible to observe the absorption of more than one optical or NIR photon during the ionization process induced by the XUV pulse [8, 10], avoiding interference effects present in similar experiments with several wavelengths of high-harmonic-generation sources [11].

The first two-color experiments with FELs detected the resulting photoelectrons angularly integrated [12, 13]. This allowed studies of the overall dependencies of the coupling between the two photon fields and the atomic system. For a more complete picture, the influence of many parameters relevant for this process have to be investigated. One of the basic parameters clearly is the emission angle of photoelectrons. By measuring the spectra angularly resolved, rich information about the dynamics of two-color photoionization can be gained [14–19].

Other fundamental parameters are the polarization states of the two intense fields. All experiments mentioned so far have been performed using linearly polarized XUV and NIR beams with their polarization directions aligned. Recently, the first two-color experiment with circularly polarized beams has been performed revealing significant circular dichroism [20]. For linearly polarized beams the important parameter is the relative orientation of the planes of polarization of the XUV and NIR pulses. Varying the relative angle between the linear polarization planes gives rise to ‘dichroic effects’, so called linear dichroism [11, 21, 22]. In paper [21] a strong dependence of the sideband amplitude on the NIR polarization was discovered for the ionization of He atoms. In this case, the initial 1s electron is excited to a p-type continuum by the XUV photon and with one additional NIR photon the final outgoing wave is a superposition of s and d states. The relative contributions of s and d waves, however, strongly depend on the orientation of the polarizations. Thus one can expect a strong dependence of the angular distribution of photoelectrons on the polarization direction. This means that changing the direction of polarization allows control over the electron emission characteristics [21]. This expectation was confirmed by theoretical calculations [23]. However, most of the experiments performed with a varying polarization

measured the angularly integrated spectrum only [21, 22]. Recently, the electron angular distribution was analyzed for the case of variable circularly polarized XUV and NIR photons [14].

Taking into account the fact that the relative angle between the polarizations can alter the angular distribution significantly, the angle-resolved measurement of the electron emission characteristics of the two-color multiphoton interaction as a function of the relative polarization angle is the next step to characterize the processes involved.

In previous angle-resolved XUV–NIR two-color experiments the linear polarizations of the two beams were parallel. In this case the photoelectron angular distribution is axially symmetric with respect to the direction of linear polarization (here the dipole approximation is assumed to be valid for the photon-atom interaction). Thus, in particular, the velocity-map-imaging (VMI) spectrometry can be applied [18, 19] for measuring the angular distribution. Introducing an additional angle between polarizations breaks the axial symmetry and the angular distribution cannot be determined easily with a VMI spectrometer anymore. In order to investigate the emission characteristics for such an asymmetric case, new detection schemes have to be applied. The direct observation of photoelectron spectra at a fixed emission angle is required. Since the initial photoionization process investigated (He (1s) and Ne (2p) ionization) yields a non-isotropic angular distribution, the scheme with only three detectors and varying NIR polarizations which was used in [17] for isotropic Auger electron emission, is also not applicable. For the present task many emission angles have to be recorded in the experiment. For this task an interaction chamber providing 16 electron time-of-flight (TOF) spectrometers symmetrically arranged in 22.5° steps which can be read out synchronously was used [24].

2. Description of experiment

The experiments were performed at the monochromator beamline PG2 [25] of the free-electron LASer in Hamburg (FLASH) [1]. For the experiments described here, the PG2 beamline was operated in 0th order. FLASH was tuned to a wavelength of 28.2 nm (44.0 eV) with a bandwidth of about 1% (<0.5 eV). This beam was focussed to a spot of ~150 μm diameter. The FEL pulse duration was estimated to be ~100 fs (FWHM) by measuring the electron bunch duration as well as the spectral statistics of the XUV beam [26, 27]. The FEL was operated in two bunch mode at 10 Hz. Every 100 ms two FEL pulses with a temporal separation of 2 μs and an average pulse energy of 50 μJ were generated. As a second radiation source the NIR laser system at FLASH [28] was used. This Ti:sapphire laser delivered 100 fs (FWHM) pulses with 0.5 mJ pulse energy at a central wavelength of 800 nm and a repetition frequency of 10 Hz. The NIR pulse was synchronized with the first FEL pulse while the second FEL pulse, which did not overlap with the NIR laser, was used to generate reference (XUV only) photoelectron spectra (see figure 1). NIR peak intensities in the order of

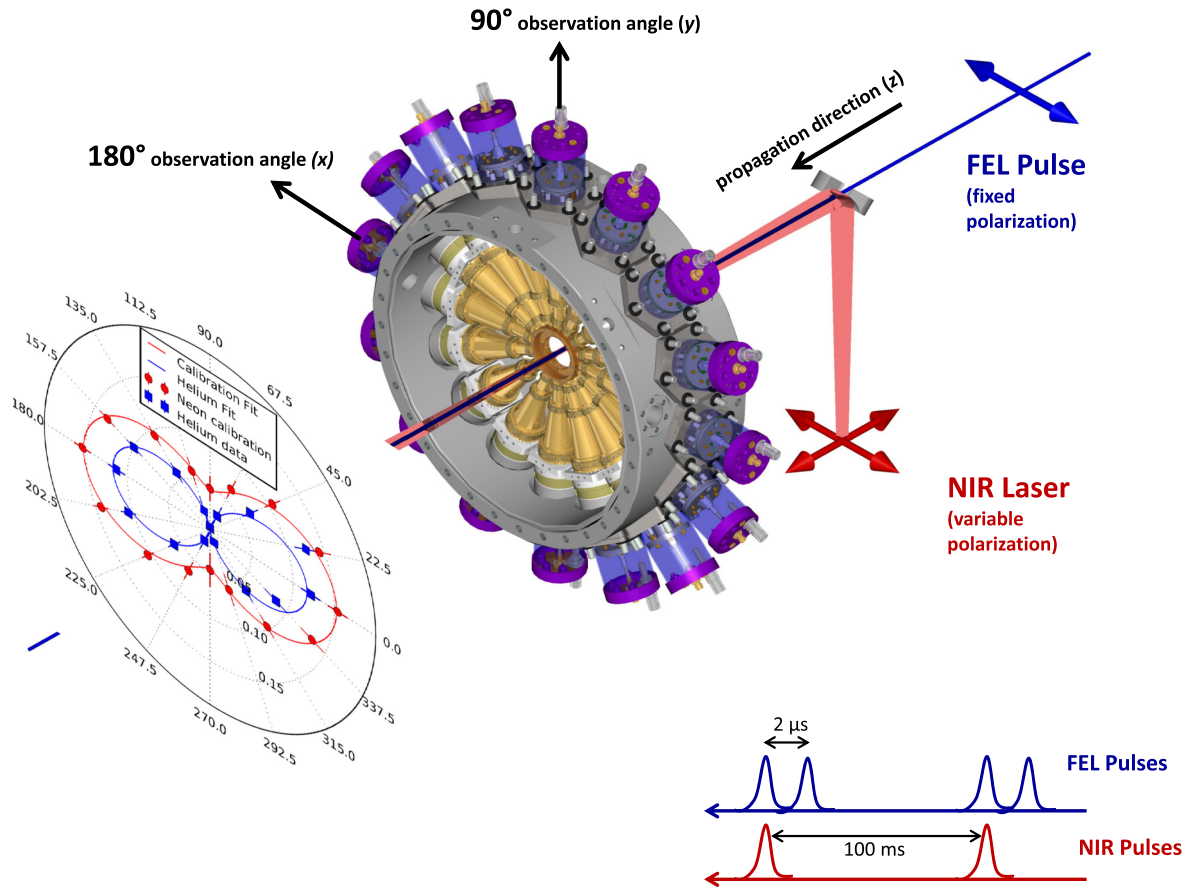


Figure 1. Schematic of the experimental setup used at the PG2 beamline of FLASH. 16 electron time-of-flight (TOF) spectrometers are arranged symmetrically in 22.5° steps around the beam. The spectrometers are mounted in the plane perpendicular to the propagation direction of the FEL and the NIR laser. NIR laser and FEL beams are overlapped using a mirror with a hole drilled through its center. While the FEL is always horizontally (linearly) polarized we rotated the polarization of the NIR laser in 15° steps. The inset on the left shows the angular distribution of the Ne and He photoelectron lines measured without NIR dressing field verifying the expected β_2 parameters. In the lower right the bunch pattern used in the experiment is schematically shown.

$10^{13} \text{ W cm}^{-2}$ were reached in the $200 \mu\text{m}$ focus. The XUV pulses were linearly polarized in the horizontal plane while the polarization of the NIR laser was rotated in 15° steps for the experiments using a true 0-order half wave plate. The NIR laser and the FEL pulses were synchronized electronically to each other with a remaining pulse to pulse jitter of ~ 100 fs (FWHM). This jitter leads to significant shot-to-shot variations of the effective NIR intensity seen by the ionized electrons. Since the recorded electron spectra for each single FEL pulse contained sufficiently well resolved spectra it was possible to subsequently sort the data according to the degree of overlap as described below. In the experimental chamber, the FEL-beam and the NIR laser are combined using a 45° mirror, with a hole in the center through which the FEL could pass, and be overlapped collinearly with a diffuse gas jet.

To measure the photoelectron spectra perpendicular to the beam, 16 TOF spectrometers were arranged in 22.5° steps around the beam as shown in figure 1 and described in [24]. The gas targets (helium or neon) were introduced through a gas needle into the center of this arrangement. The resulting photoelectron spectra are read out simultaneously with 16 analog to digital converter (ADC) channels based on μTCA technology. ADC traces were recorded for each single FEL

pulse at a repetition frequency of 10 Hz using a sample rate of 4 GS s^{-1} and a vertical resolution of 12 bits [31]. As alluded to above, only every second FEL pulse overlapped temporally and spatially with the NIR pulse leading to a large number of ‘FEL-only’ reference spectra. These were used to analyze the detector response function in order to remove the spurious high frequency ringing that followed the fast (≤ 1 ns) micro channel plate detector pulse. In addition, detector cross talk was strongly reduced in post processing by a covariance matrix analysis [29, 30]. Finally, this reference spectrum was used to verify the correct operation of the TOF setup by the determination of the angular distribution of the ‘undressed’ photoelectrons as shown in figure 1. The angular distribution anisotropy parameter (β_2) was determined to be 0.88 ± 0.14 for neon and 1.94 ± 0.1 for helium. These values are in good agreement with the reference values of $\beta_2(44 \text{ eV}) \sim 0.9$ and $\beta_2(44 \text{ eV}) = 2.0$ for neon and helium, respectively [32].

Using the TOF position of the main photoline for opposite detectors, one can extract the position of each single FEL shot from the spectra. Due to pointing instabilities, the FLASH focus moved randomly with a RMS-jitter of about $60 \mu\text{m}$. This made an accurate overlap between NIR laser and FEL challenging. To minimize the fluctuation of the overlap

in the analyzed data, the overlap was identified individually for each recorded spectrum. The relative amplitude of the sidebands with respect to the main line was determined and used as a measure for the degree of overlap. For the further analysis only 10% of the recorded spectra yielding the highest degree of overlap were taken into account as previously reported in [18].

3. Simulation of the interaction

To interpret the experimental results, simulations have been performed using a theoretical approach based on the strong-field approximation (SFA) [33], which is presented in detail in [34]. The model describes the ionization by the XUV pulse in an ‘undressed’ free atom, but the emitted ‘free’ photoelectrons, propagating from the atom to the detector, interact with the strong NIR field which affects the electron energy as well as the scattering angle. In this approximation, the photoelectron is described by the Volkov wave function [35] which contains all partial waves with corresponding field-modified phases. For photoelectron energies of several tens of eV, as is the case here, this approach describes experimental results [17, 18, 20] as well as the results of much more elaborate calculation methods based on the time-dependent Schrödinger equation [36–38]. The angle between polarization planes was varied from 0° to 90° in 15° steps for collinear beams, as in the experiment. The photoelectron energy and angular distribution (double differential cross section) was calculated for emission in the plane perpendicular to the beam direction. The relevant dipole matrix elements and phases have been calculated within the Hartree–Slater approximation [39], which provides the angular distribution parameter for one-photon absorption and has previously shown good agreement with experiments [40].

The SFA calculations were performed for ten different NIR laser peak intensities between zero and $8.0 \times 10^{12} \text{ W cm}^{-2}$ for a 80 fs NIR (flat-top) pulse with a center wavelength of 800 nm. The FEL pulse with a wavelength of 28.2 nm (44 eV) was simulated as a 10 fs Gaussian pulse corresponding to a single SASE mode of the FLASH FEL. Thus the ionization process happens in the simulation for a well defined NIR intensity. It is on the other hand known from the experimental conditions that the pulse duration and focal spot for the NIR laser pulse and the FEL pulse are similar, and there is temporal and spatial jitter. This leads to a broad effective NIR intensity distribution that affects the ionization process. In order to simulate the actual experiment, the weight for each NIR intensity was determined by a model that takes the measured focal spot sizes and pulse durations into account. This model yields a weighting factor for each constant peak intensity. In addition, careful analysis of the experimental data showed that the spatial overlap of the FEL and the NIR laser pulses was not ideal and fluctuations from pulse to pulse were also taken into account for the weighting procedure.

Naturally, this is a rather rough approximation since in reality the XUV pulse has a very complicated temporal shape which is different from shot to shot [26]. Therefore, one can only expect a qualitative agreement of the simulation with experiment.

4. Results and discussion

The electron TOF spectra were recorded for 16 angles (in 22.5° steps) perpendicular to the propagation direction of the FEL for different orientations of the polarization plane of the co-propagating NIR laser. In the experiment seven different laser polarization angles (in 15° steps) were used. The polarization plane of the NIR laser was rotated from parallel polarization of the FEL and the NIR laser (0°) to perpendicular polarization (90°). The TOF spectra measured for different observation angles and NIR polarizations yields a four-dimensional data set. In order to display the data in an appropriate way and to compare them to the simulation results, the data have to be projected. The spectra are shown separately for each observation angle as function of the NIR polarization. This way was chosen because the multiphoton processes involve several sidebands leading to a complex angular distribution. In an interaction resulting in n sidebands a minimal number of n NIR photons are involved, leading to oscillatory structures in the angular distribution which have to be described with Legendre polynomials up to $2(n + 1)$ order [18, 34, 41]. For a comprehensive measurement of such complex structures an even higher angular resolution is needed. For the limited amount of eight spectrometers per hemisphere employed here it is better to present the data for a fixed emission angle as a function of the angle of the NIR laser polarization with respect to the FEL polarization.

For an FEL photon energy of 44 eV helium was ionized from the 1s shell with a binding energy of 24.6 eV [42] resulting in a main photoelectron line (without NIR laser) with a kinetic energy of 19.4 eV. The unperturbed angular distribution of the He (1s) line has a beta parameter of $\beta_2 = 2$. For neon on the other hand the Ne (2p) shell is ionized leading to a distinctly different angular distribution with a beta parameter of $\beta_2 \sim 0.9$ [32]. The Ne (2p) state is split into Ne $2p_{1/2}$ and Ne $2p_{3/2}$ states with a binding energy of 21.7 eV and 21.6 eV, respectively. Due to the bandwidth of the FEL (~ 0.4 eV), the splitting is not resolved. The unperturbed photoionization line for neon is thus at a kinetic energy of 22.4 eV.

Representative experimental and simulated results for He (1s) and Ne (2p) are shown in figures 2 and 3, respectively, displayed as TOF spectra as a function of the NIR laser polarization angle for the individual emission angles. The experimental conditions for two opposite TOF spectrometers are identical for symmetry reasons and yield identical TOF traces. This assumption was carefully checked and is fulfilled in the experiment.

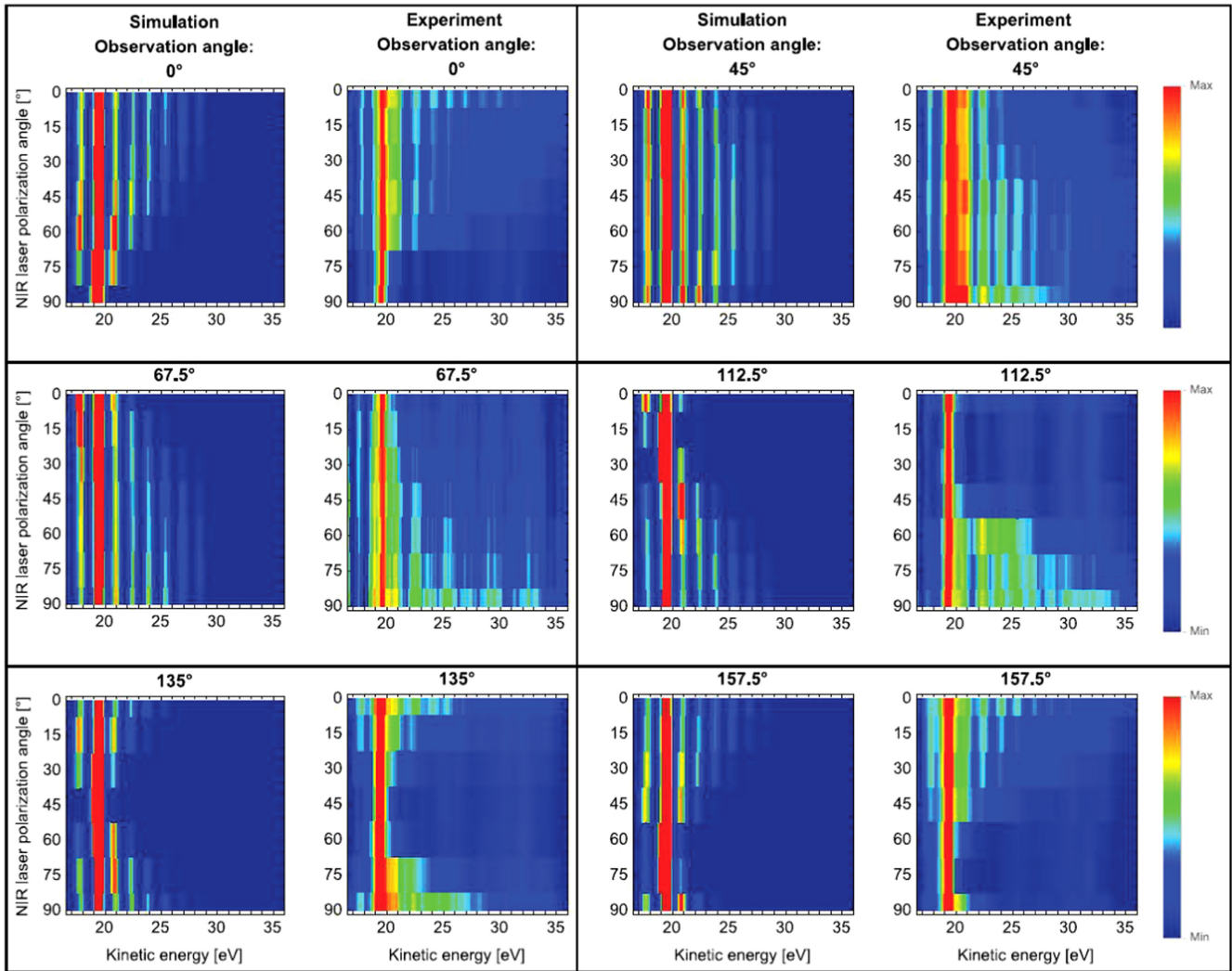


Figure 2. The angularly resolved spectra of helium 1s electrons photoionized at an FEL wavelength of 28.2 nm (44 eV) in the presence of an intense (peak intensity $\sim 10^{13}$ W cm $^{-2}$) NIR laser field are shown. Besides the unperturbed main photoionization line (at 19.4 eV) several NIR induced sidebands are visible showing a strong dependence on the NIR polarization angle as well as on the emission angle. The photoelectron spectra are displayed as a function of the plane of the polarization of the NIR laser. The experimental as well as the simulated spectra are shown for six different observation angles perpendicular to the propagation direction of the FEL/NIR laser. All spectra are shown in the same color scale and are normalized on maximum and minimum values.

The number of observed sidebands varies strongly with the polarization direction of the NIR laser. It is different also for the different observation directions. The main photoionization line in contrast is present for all laser polarization angles which is attributed to the FEL focal spot fluctuations leading to atoms which are outside the NIR focus and thus emitting ‘undressed’ electrons. Simulations for constant NIR intensities (no undressed electrons) would lead us to conclude that depletion of the main photoline should be very significant [18].

We consider the case of parallel polarizations of the FEL and the NIR pulses (NIR polarization angle of 0°). Here, at an observation angle of 0° the number of sidebands is highest while for higher angles towards the observation direction perpendicular to the NIR polarization direction the spectra show fewer sidebands in agreement with [18]. This is easily

explained by the fact that the interaction of an electron, emitted at a certain direction with respect to the IR field, is determined by the projection of the field on this direction. If an electron moves close to the perpendicular direction to the field, it does not interact with the field and no sidebands are formed. Similarly, for other angles between polarizations, the maximum number of sidebands is formed when the NIR polarization is directed towards the respective detector, i.e. along the electron linear momentum (see figure 2 as well as figure 3). This observation holds for the simulation as well as for the experiment.

The angular distribution of a particular sideband is in general determined by two factors: a primary angular distribution in XUV photoionization and modification of this distribution by the NIR field. For the comparatively large intensity of the NIR field considered in this paper, which

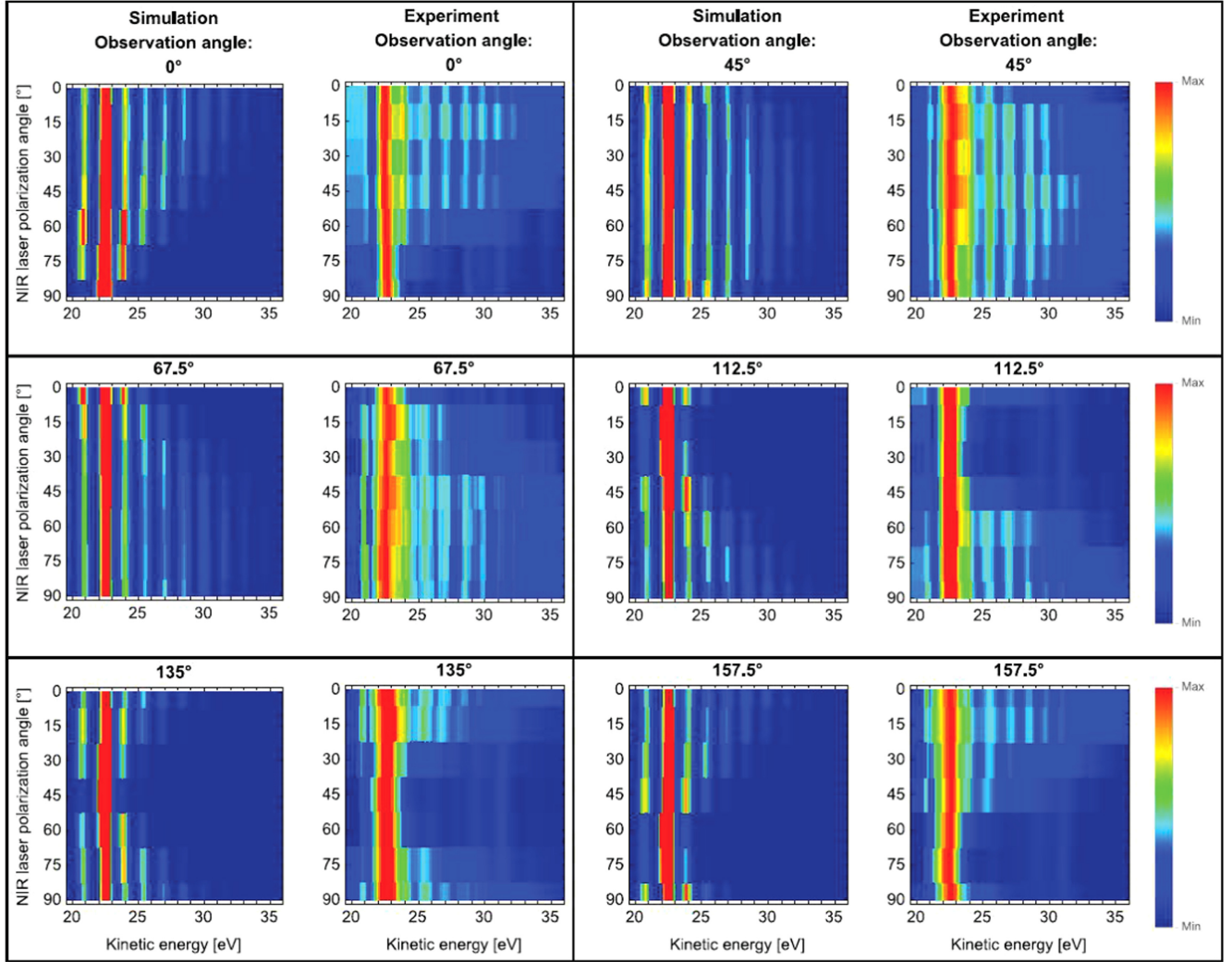


Figure 3. The angularly resolved spectra of neon 2p electrons photoionized at an FEL wavelength of 28.2 nm (44 eV) in the presence of an intense (peak intensity $\sim 10^{13}$ W cm $^{-2}$) NIR laser field are shown. Besides the unperturbed main photoionization line (at 22.4 eV) several NIR induced sidebands are visible showing a strong dependence on the NIR polarization angle as well as on the emission angle. The photoelectron spectra are displayed as a function of the plane of the polarization of the NIR laser. The experimental as well as the simulated spectra are shown for six different observation angles perpendicular to the propagation direction of the FEL/NIR laser. All spectra are shown in the same color scale and are normalized on maximum and minimum values.

leads to a large number of sidebands, the second factor is dominant. Indeed, despite the different angular distribution in one-photon XUV ionization for He (1s) with $\beta_2 = 2$ and Ne (2p) with $\beta_2 \sim 0.9$, the measured and simulated emission characteristics of entire process as shown in figures 2 and 3 are almost identical. The large number of absorbed NIR photons mainly define the angular distribution of the sidebands. In addition, this distribution depends on the kinetic energy of the electrons. In the present case, the kinetic energies of He (1s) and Ne (2p) are similar enough that the observed sideband distributions are indeed almost identical.

The detailed behavior of the sideband intensity as a function of the angle between polarizations can be qualitatively understood using an approximate expression for the intensity of the m th sideband, obtained in [23] within the SFA for the s-shell ionization (see expression (A24) in the appendix to that paper) which reflects the influence of the

NIR field on the electron energy and angular distribution:

$$\sigma^{(m)} \sim |J_m(\bar{q})|^2 \sin^2 \vartheta \cos^2 \varphi, \quad (1)$$

where ϑ , φ are emission angles of the photoelectron (we remind the reader that z -axis is along the beam direction, x -axis is along the XUV polarization), $J_m(\bar{q})$ is the Bessel function. Here

$$\bar{q} = \frac{A_L k}{\omega_L} \sin \vartheta \cos(\phi - \chi), \quad (2)$$

where A_L and ω_L are the vector potential and fundamental frequency of the NIR field, respectively, k is the linear momentum of the electron and χ is the angle between polarizations. A similar expression has been obtained earlier in [21] on the basis of the ‘soft photon’ approximation [43]. In the considered case when electrons are detected in the plane perpendicular to the beam direction, $\vartheta = 90^\circ$. For a certain direction of electron emission φ , and fixed other parameters,

the maximum intensity is achieved when $\chi = \varphi \pm \pi$, i.e. when an electron is emitted along the direction of NIR polarization. This condition corresponds to the maximum number of observed sidebands as noted above. On the contrary, when $\chi = \varphi + \pi/2 \pm \pi$ the argument of the Bessel function $\bar{q} = 0$, therefore, the intensity of all sidebands is zero and only the central line ($m = 0$) survives. This is clearly seen in figure 2 where for an observation angle of 0° and a NIR field direction of 90° only the main line is observed.

In the considered case the dimensionless prefactor $\frac{A_L k}{\omega_L}$ in equation (2) is about ~ 5.5 , therefore, with variation of the NIR polarization angle, the argument of the Bessel function changes in the interval from 0 to 5.5. From the properties of Bessel functions it follows that the intensity of sidebands with $m = 1 - 4$ as a function of χ is non-monotonic, it reaches a maximum at some angle and then decreases. This is clearly seen in figure 2. For sidebands of larger order, the intensity changes monotonically with χ .

We note that due to similarity of the results for He(1s) and Ne(2p) ionization, qualitatively, the above discussed characteristics of the distributions are valid also for Ne(2p).

5. Conclusion

In conclusion, the two-color multiphoton interaction of XUV FEL and NIR femtosecond pulses with helium and neon targets was investigated. The formation of sidebands in the photoelectron spectrum was recorded angularly resolved as a function of the relative angle of polarization between the XUV and the NIR fields. Sixteen electron TOF spectrometers symmetrically arranged perpendicular to the propagation direction of the XUV/NIR beams measured the resulting sideband distribution. It was shown that in contrast to low NIR intensities, for high intensities the angular distribution of the sidebands is to a large extent dominated by the polarization direction of the NIR field covering the initial angular distribution of the XUV ionization. The processes were simulated within the SFA which yielded a consistent agreement between experiment and simulation. This first angularly resolved measurement of the generation of sidebands as a function of the polarization angle of the NIR dressing field supports the understanding of the complex multiphoton processes.

Acknowledgments

We want to acknowledge the work of the scientific and technical team at FLASH. NMK acknowledges hospitality and financial support from FS-DESY as well as from the theory group in cooperation with the SQS work package of European XFEL (Hamburg) and the financial support of the Russian Ministry of Education and Science within the program 'Physics with Accelerators and Reactors in West Europe'. MM and TM acknowledge the support by the Deutsche

Forschungsgemeinschaft (DFG) under grant nos. SFB925/A1 and SFB925/A3. TJK and JC acknowledge support by Science Foundation Ireland grant no. 12/IA/1742. PJ acknowledges the support from the Swedish Research Council and the Swedish Foundation for Strategic Research. MI acknowledges funding of the Volkswagen Foundation within a Peter Paul Ewald-Fellowship.

References

- [1] Ackermann W *et al* 2007 *Nat. Photon.* **1** 336
- [2] Emma P *et al* 2010 *Nat. Photon.* **4** 641
- [3] Ishikawa T *et al* 2012 *Nat. Photon.* **6** 540
- [4] Allaria E *et al* 2012 *Nat. Photon.* **6** 699
- [5] Richter M, Bobashev S V, Sorokin A A and Tiedtke K 2010 *J. Phys. B: At. Mol. Opt. Phys.* **43** 194005
- [6] Berrah N *et al* 2010 *J. Mod. Opt.* **57** 1015
- [7] Bostedt C *et al* 2013 *J. Phys. B: At. Mol. Opt. Phys.* **46** 164003
- [8] Meyer M, Costello J T, Dusterer S, Li W B and Radcliffe P 2010 *J. Phys. B: At. Mol. Opt. Phys.* **43** 194006
- [9] Glover T E, Schoenlein R W, Chin A H and Shank C V 1996 *Phys. Rev. Lett.* **76** 2468
- [10] Radcliffe P *et al* 2012 *New J. Phys.* **14** 043008
- [11] O'Keefe P, López-Martens R, Mauritsson J, Johansson A, L'Huillier A, Vénier V, Taieb R, Maquet A and Meyer M 2004 *Phys. Rev. A* **69** 051401
- [12] Meyer M *et al* 2006 *Phys. Rev. A* **74** 011401(R)
- [13] Radcliffe P *et al* 2007 *Appl. Phys. Lett.* **90** 131108
- [14] Mazza T *et al* 2015 *J. Electron Spectrosc. Relat. Phenom.* **204** 313
- [15] Guyétand *et al* 2005 *J. Phys. B: At. Mol. Opt. Phys.* **38** L357
- [16] Haber L H, Doughty B and Leone S R 2009 *J. Phys. Chem. A* **113** 13152
- [17] Haber L H, Doughty B and Leone S R 2011 *Phys. Rev. A* **84** 013416
- [18] Meyer M *et al* 2012 *Phys. Rev. Lett.* **108** 063007
- [19] Dusterer S *et al* 2013 *J. Phys. B: At. Mol. Opt. Phys.* **46** 164026
- [20] Mondal S *et al* 2014 *Phys. Rev. A* **89** 013415
- [21] Mazza T *et al* 2014 *Nat. Commun.* **5** 3648
- [22] Meyer M *et al* 2008 *Phys. Rev. Lett.* **101** 193002
- [23] Richardson V, Li W B, Kelly T J, Costello J T, Nikolopoulos L A A, Dusterer S, Cubaynes D and Meyer M 2012 *J. Phys. B: At. Mol. Opt. Phys.* **45** 085601
- [24] Kazansky A K, Grigorieva A V and Kabachnik N M 2012 *Phys. Rev. A* **85** 053409
- [25] Allaria E *et al* 2014 *Phys. Rev. X* **4** 041040
- [26] Gerasimova N *et al* 2011 *J. Mod. Opt.* **58** 1480
- [27] Dusterer S *et al* 2014 *Phys. Rev. STAB* **17** 120702
- [28] Engel R, Dusterer S, Brenner G and Teubner T 2016 *J. Synchrotron Radiat.* **23** 118
- [29] Redlin H *et al* 2011 *Nucl. Instrum. Methods A* **635** 88
- [30] Frasniski L J, Codling K and Hatherly P A 1989 *Science* **246** 1029
- [31] Frasniski L J *et al* 2013 *Phys. Rev. Lett.* **111** 073002
- [32] <http://spdevices.com/index.php/adq412>
- [33] Becker U and Shirley D (ed) 1996 *VUV and Soft X-ray Photoionization* (New York: Plenum)
- [34] Keldysh L V 1965 *Sov. Phys.—JETP* **20** 1307
- [35] Kazansky A K, Sazhina I P and Kabachnik N M 2010 *Phys. Rev. A* **82** 033420
- [36] Wolkow D M 1935 *Z. Phys.* **94** 250
- [37] Kazansky A K and Kabachnik N M 2006 *J. Phys. B: At. Mol. Opt. Phys.* **39** 5173

- [37] Kazansky A K and Kabachnik N M 2007 *J. Phys. B: At. Mol. Opt. Phys.* **40** 2163
- [38] Kazansky A K and Kabachnik N M 2007 *J. Phys. B: At. Mol. Opt. Phys.* **40** 3413
- [39] Herman F and Skillman S 1963 *Atomic Structure Calculations* (Englewood Cliffs, NJ: Prentice-Hall)
- [40] Kennedy D J and Manson S T 1972 *Phys. Rev. A* **5** 227
- [41] Bauch S and Bonitz M 2008 *Phys. Rev. A* **78** 043403
- [42] Thompson A C *et al* 2001 *X-ray Data Booklet* (Berkeley, CA: Lawrence Berkeley National Laboratory) (<http://xdb.lbl.gov/>)
- [43] Maquet A and Taieb R 2007 *J. Mod. Opt.* **54** 1847